

Numerical and experimental analysis of autoignition induced by shock wave focusing

Zezhong Yang, Bo Zhang
Shanghai Jiao Tong University
Shanghai, China

1. Introduction

The ignition phenomenon is one of the most important characteristics of combustion. Over the past decades, considerable studies on the auto-ignition behavior behind the reflected shock wave in shock-tube experiments have been undertaken. Two ignition modes are identified by Voevodsky and Soloukhin[1]: weak ignition and strong ignition, which are also known as mild ignition and sharp ignition. Strong ignition refers to a blast wave that is homogeneously formed at the end wall of the shock tube[2]. Strehlow and Cohen[3] described the blast wave as the coupling of the shock wave and reaction zone. Petersen with coworkers[4] considered it as a detonation-like structure with a sharp increase in pressure. Compared with strong ignition, weak ignition is much more complex: flame kernels appear behind the reflected shock wave and finally emerge to form a uniform flame front which can be considered as deflagration. In some cases, DDT (deflagration-to-detonation transition) takes place with the acceleration of the flame front[5,6]. The direct transition from the flame kernel into detonation is also observed in acetylene-oxygen mixture[7]. The formation process of the flame kernels is clearly observed in recent studies[8] and the flame kernel occurrences are mainly due to the temperature inhomogeneity behind the reflected shock wave.

Since the ignition mode is highly correlated with the intensity of the incident shock wave, determining how to obtain detonation reliably with weak incident shock wave has become a hot topic in the past two decades. This study investigates the autoignition induced by the shock wave focusing with two wedge reflectors of different angles (a 60° wedge reflector and a 90° wedge reflector), which have also been employed in our previous study[9]. Methane-oxygen mixture has been applied because it is a hydrocarbon fuel which is widely used in shock-tube experiments, and thus considerable reference data is available. The same intensity of the incident shock wave is employed in different reflectors to study the effect of wedge angle on shock wave focusing and ignition mode. Small flow instability structures captured both in experiments and simulations are analyzed. The ignition and flame propagation modes induced by incident shock waves with different Mach numbers of the incident shock waves (M_{si}) are discussed systematically.

2. Experimental and simulation setup

In this study, the experiments are carried out in a double-diaphragm shock tube as shown in Fig. 1. The tube is composed of three parts: a 1-meter-long driver section, a 1-meter-long driven section, and a 0.1-meter-long double diaphragm section. The cross-section of the tube is a 40 mm \times 73 mm rectangle. The schlieren viewing window is installed at the end of the driven section with a size of 200 mm \times 73 mm. In this experiment, two different angle wedges are tested: 60° and 90°. Both wedges' apexes have been cut off to form a 7 mm width plane to install a piezoelectric pressure transducer (PT5). Other transducers (PT1 – PT4) are installed along the sidewall of the driven section. The detailed positions are shown in Fig. 1. A PicoScope 4824 oscilloscope is utilized to record the waveform with a sampling frequency of 200 kHz. To visualize the ignition procedure, the Z-type schlieren system equipped with a high-speed camera (Phantom V710L) is employed at the quartz window. The camera has a frame rate of 100,000 frames per second and a resolution of 320 \times 120 px².

The finite-volume open-source OpenFOAM-v2006 is employed, and the solver developed by Kraposhin et al.[10] is utilized in the simulation part. This solver is widely used in supersonic combustion, especially in the field of detonation, and the accuracy of the numerical scheme in the simulation is 2nd order both in time and space. 20 μ m is chosen as the smallest grid size for the simulation to strike a balance between the simulation's accuracy and computation time.

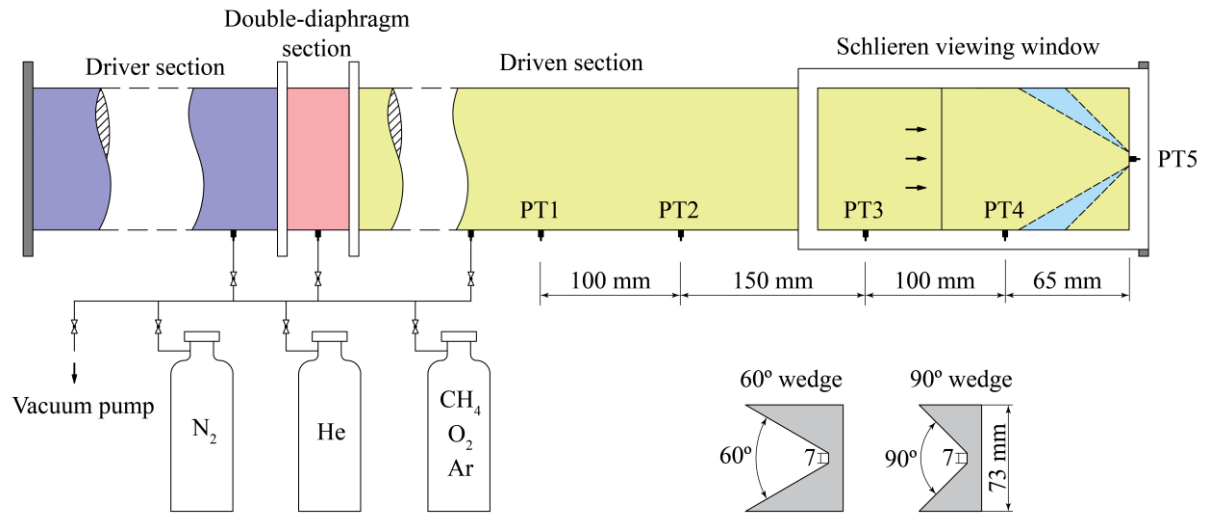


Figure 1: Schematic diagram of the experimental facilities

3. Results and discussion

The comparison of the numerical and experimental schlieren images is shown in Fig. 2. The incident shock wave propagates into the wedge at $t = 39 \mu$ s. At $t = 79 \mu$ s, the shock wave reflects over the wedge surface and forms pseudo-steady transition-Mach reflection (TMR) [11]. Considering the reflection type, the two triple points will merge at the center axis before reaching the top plane of the reflector, creating a high pressure and temperature region after the merged shock wave. The ignition starts at the end-wall region due to the head-on collision of the shock wave and the wedge at $t = 109 \mu$ s. Consequently, the flame front propagates toward the driver section part, coupled with the reflected shock wave, and hence can be considered as a curved detonation wave. Unlike other ignition combustion studies, the bright shining light emitted by the wave indicates that the intense combustion is ongoing, providing a strong support that this combustion wave is detonation wave. Due to shock wave boundary layer interaction (SWBLI), the part of the reflected shock which is in contact with the tube wall shows a significant bending (red dashed circle at $t = 159 \mu$ s). This flow structure has been clearly captured both in experiments and simulations. At $t = 179 \mu$ s, the detonation wave passes through the wedge reflector

region and enters the straight tube section. Due to the Mach reflection, the near-wall part of the curved detonation wave become almost perpendicular to the tube wall.

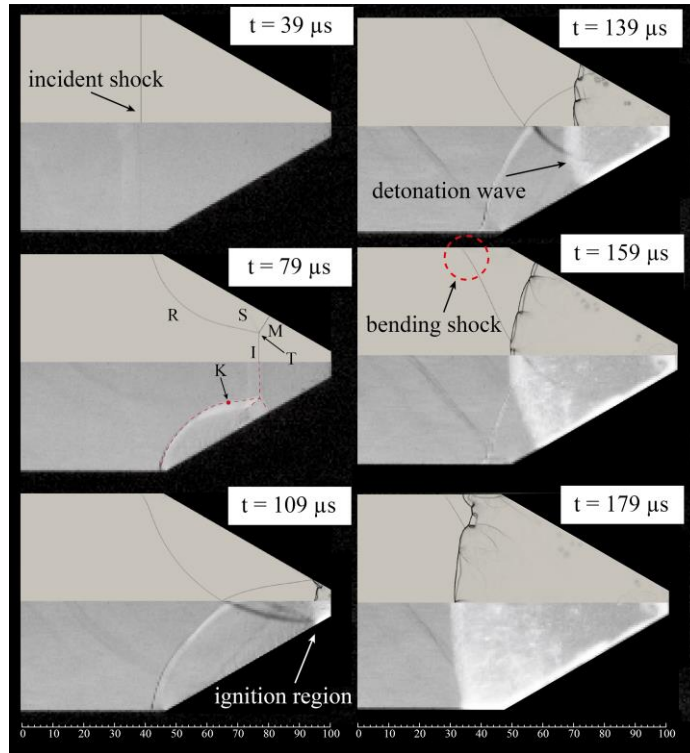


Figure 2: Comparison of the numerical (upper half) and experimental (lower half) schlieren images under the condition of $M_{si} = 3.30$. I: incident shock wave, R: reflected shock wave, M: Mach stem, S: slipstream, K: kink point, T: triple point

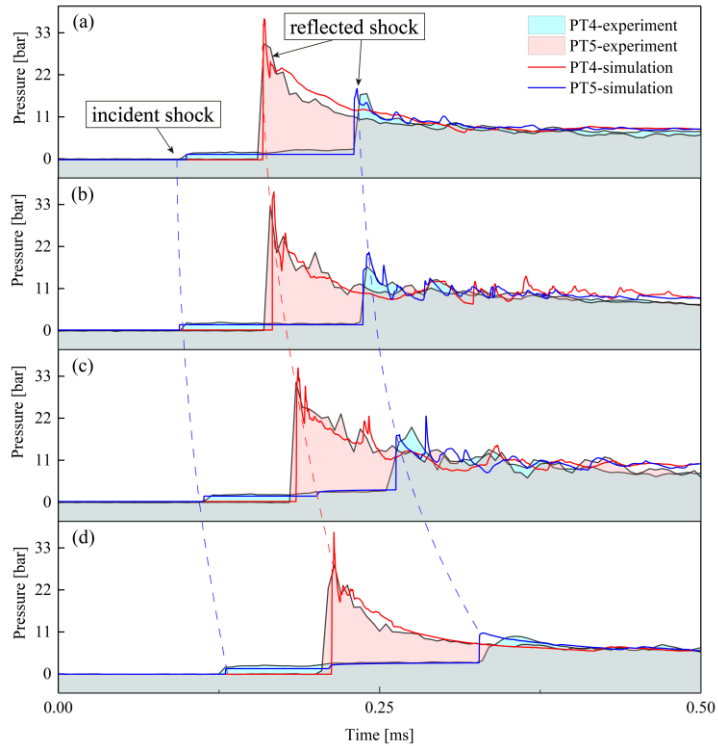


Figure 3: Comparison of the numerical and experimental pressure signals of PT4 and PT5 in a 60° wedge reflector. (a) $M_{si} = 3.30$ (b) $M_{si} = 3.17$ (c) $M_{si} = 2.80$ (d) $M_{si} = 2.42$

Figure 3 shows the comparison of the experimental signals recorded by pressure transducers PT4 and PT5 and the signals recorded by virtual probes set exactly at the same place in simulations. Zero of the x -coordinate is when PT3 detects the arrival of incident shock wave. The simulation's results are in line with the experiment, particularly the pressure measured after the flame front passes the transducers (time after the second dashed blue curved line in Fig. 3). The maximum time difference is nearly 3.8%, while the pressure difference between numerical and experimental data is normally lower than 5%. However, the highest discrepancy between the peak pressure values measured by PT5 is roughly 30% in Fig. 3(d). This mismatch could be attributed to the numerical oscillation at the end wall, which is caused by an excessive time step. With the time step becomes smaller, the oscillation quickly dampens to the normal value. Therefore, it can be assumed that it has no appreciable impact on the numerical results.

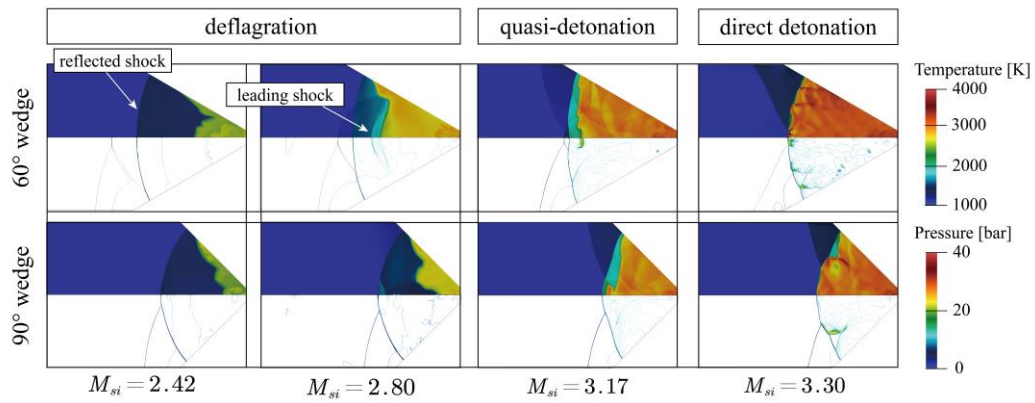


Figure 4: Comparison of shock wave focusing performance of a 60° wedge reflector and a 90° wedge reflector with different incident shock wave intensity. Temperature contour (up), pressure contour (down)

Figure 4 shows a systematic investigation of the shock wave focusing performance of a 60° wedge reflector and a 90° wedge reflector with different incident shock wave intensities. The images where the shock waves are almost at the same position are chosen to be compared. With the Mach number increasing from 2.42 to 3.30, the flame temperature increases as well. Under the conditions of $M_{si} = 2.42$ and $M_{si} = 2.80$, no detonation wave is generated. However, in a 60° wedge reflector, the deflagration wave is much faster than the wave in a 90° wedge reflector in the same intensity. In particular, a leading shock is formed before the flame at $M_{si} = 2.80$, which shows a possibility of transiting into a detonation wave. However, DDT fails in this case. Under the condition of $M_{si} = 3.17$, flames in both reflectors propagate in quasi-detonation mode, while flames propagate in direct detonation mode at $M_{si} = 3.30$. The number of transverse waves in the 60° wedge reflector is more than in the 90° wedge reflector, demonstrating that the detonation wave is in a more stable propagation mode. Therefore, a 60° wedge reflector turns out that it has better shock wave focusing performance than a 90° wedge reflector.

A mushroom-shaped jet is observed at the apex of the wedge reflector, as shown in Fig. 5(a-c). However, the jet in Fig. 5(d) is not well formed, which may be due to the flow disturbance and fluctuation after the reflected shock wave. It is interesting that this small flow instability structure only appears in the cases where detonation waves are successfully formed. The simulation in Fig. 6, which corresponds to the experiment condition shown in Fig. 5(a), may enhance the comprehension of this phenomenon. The numerical schlieren image (Fig. 6(a)) shows the same flow instability structure. It seems that the spike of the mushroom-shaped jet is more developed in simulation and a second small spike arises due to the Richtmyer-Meshkov instability. The temperature of the mushroom-shaped jet (Fig. 6(b)) is higher than the surrounding region, indicating that the reaction is more intense in the jet region. Assuming that the vorticity is generated post-shock at the intersection of the shock and interface and neglecting the

viscous effect, then we get the baroclinic equation: $|d\boldsymbol{\omega} / dt| = |(\nabla\rho \times \nabla p) / \rho^2|$, which indicates the magnitude of the misalignment between the density gradient and the pressure gradient. The baroclinic effect induces a pair of vortices which form the mushroom shape and promote the turbulent mixing of the jet. As shown in Fig. 6(d), the O_2 mass fraction in the jet is much higher than in the surrounding region. This demonstrates that a very small part of the mixture has not been ignited, or been weakly ignited, at the stage of detonation formation. The mixture remains in the center region of the top plane. After a few microseconds, the ignition starts due to the uprising temperature behind the detonation wave, and the turbulent mixing caused by the baroclinic effect promotes the combustion of the jet. The remaining of the unburnt mixture is probably due to the premature collision of the triple points before reaching the top plane of the wedge reflector, creating an unburnt mixture bubble at the end wall.

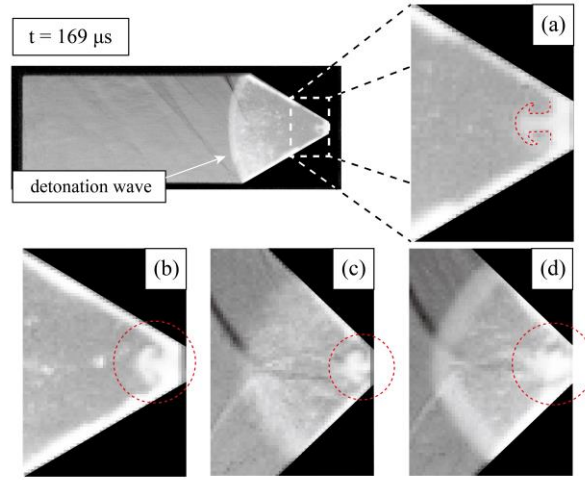


Figure 5: Flow instability near the apex plane of the reflector (a) $M_{si} = 3.30$, 60° wedge reflector (b) $M_{si} = 3.17$, 60° wedge reflector (c) $M_{si} = 3.17$, 90° wedge reflector (d) $M_{si} = 3.30$, 90° wedge reflector

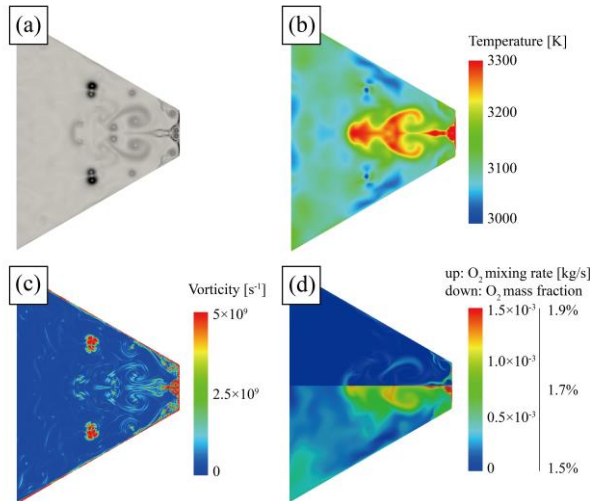


Figure6: Simulation under the condition of $M_{si} = 3.30$ in a 90° wedge reflector (a) numerical schlieren (b) temperature contour (c) vorticity contour (d) mixing rate of O_2 (up) and contour of O_2 mass fraction (down), mixing rate = $|\mu \nabla \cdot Y_{O_2}|$

4. Conclusions

In this study, experimental and numerical studies are carried out to study the ignition induced by shock wave focusing with two wedge reflectors of different angles. The different ignition modes under various incident shock wave intensities and reflectors are examined. The detonation initiation and self-sustaining mechanisms are analyzed. A small flow instability structure is observed in both the experiment and simulation. The results are summarized as follows:

- 1) A comprehensive comparison of computational and experimental parameters, including pressure signals and schlieren images, reveals that the error is within a reasonable range, which demonstrates that the simulation results are credible.
- 2) Three ignition modes (deflagration, quasi-detonation, and direct detonation) generally exist in wedge reflectors. The ignition modes are highly affected by the intensity of the shock wave. Furthermore, the 60° wedge reflector shows a better detonation-initiation effect.
- 3) The formation of new hot spots and transverse waves is crucial to the self-sustaining of the detonation initiated by focused shock in the wedge reflector. The decoupling of the detonation wave is mainly due to the negative concentration gradient of the combustible mixture before the detonation wave.
- 4) A mushroom-shaped jet caused by Richtmyer-Meshkov instability is observed in all detonation cases, which means that the jet is an important feature of successful generation of a detonation wave.

References

- [1] Voevodsky VV, Soloukhin RI. On the mechanism and explosion limits of hydrogen-oxygen chain self-ignition in shock waves. *Symposium (International) on Combustion* 1965;10:279–83.
- [2] Grogan KP, Ihme M. Weak and strong ignition of hydrogen/oxygen mixtures in shock-tube systems. *Proceedings of the Combustion Institute* 2015;35:2181–9.
- [3] Strehlow RA, Cohen A. Initiation of Detonation. *The Physics of Fluids* 1962;5:97–101.
- [4] Petersen EL, Davidson DF, Hanson RK. Ignition Delay Times of Ram Accelerator CH/O/Diluent Mixtures. *Journal of Propulsion and Power* 1999;15:82–91.
- [5] Meyer JW, Oppenheim AK. On the shock-induced ignition of explosive gases. *Symposium (International) on Combustion* 1971;13:1153–64.
- [6] Zhang B. The influence of wall roughness on detonation limits in hydrogen–oxygen mixture. *Combustion and Flame* 2016;169:333–9.
- [7] Yamashita H, Kasahara J, Sugiyama Y, Matsuo A. Visualization study of ignition modes behind bifurcated-reflected shock waves. *Combustion and Flame* 2012;159:2954–66.
- [8] Merkel AC, Ciccarelli G. Visualization of lean methane-air ignition behind a reflected shock wave. *Fuel* 2020;271:117617.
- [9] Gelfand BE, Khomik SV, Bartenev AM, Medvedev SP, Grönig H, Olivier H. Detonation and deflagration initiation at the focusing of shock waves in combustible gaseous mixture. *Shock Waves* 2000;10:197–204.
- [10] Kraposhin M, Bovtrikova A, Strijhak S. Adaptation of Kurganov-Tadmor Numerical Scheme for Applying in Combination with the PISO Method in Numerical Simulation of Flows in a Wide Range of Mach Numbers. *Procedia Computer Science* 2015;66:43–52.
- [11] Ben-Dor G. A State-of-the-Knowledge Review on Pseudo-Steady Shock-Wave Reflections and their Transition Criteria. *Shock Waves* 2006;15:277–94.